Supplementary Information for:

Breakdown of Ohm's Law by Disorders in Low-Dimensional Transistors

Chang Niu, Adam Charnas, Jian-Yu Lin, Linjia Long, Zehao Lin, Zhuocheng Zhang and Peide D. Ye*

Elmore Family School of Electrical and Computer Engineering and Birck Nanotechnology Center, Purdue University, West Lafayette, IN 47907, United States.

*Correspondence and requests for materials should be addressed to P. D. Y. (yep@purdue.edu)

List of contents:

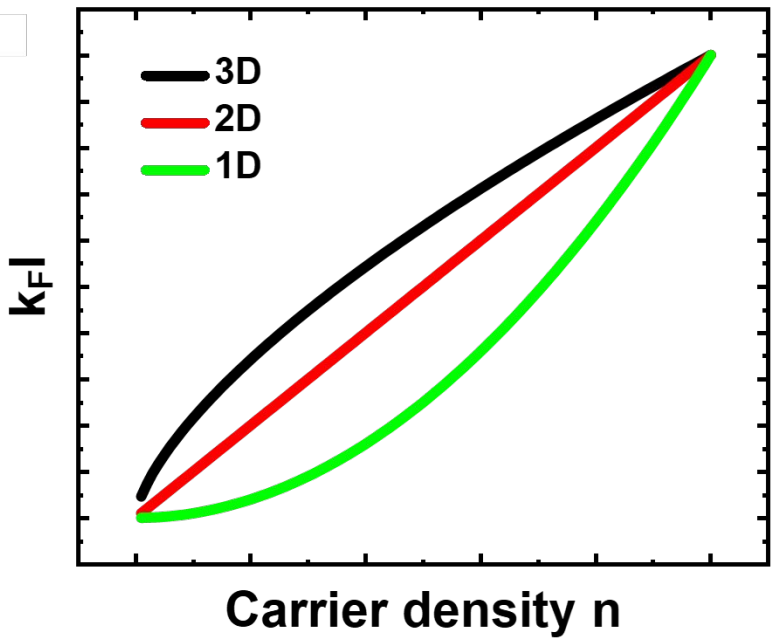

Figure S1. Degree of disorder scaling with carrier density in different dimensions. With decreasing dimensionality, the degree of disorder scales more rapidly with carrier density, indicating that disorder effects become increasingly pronounced and influential in lower-dimensional transistors.

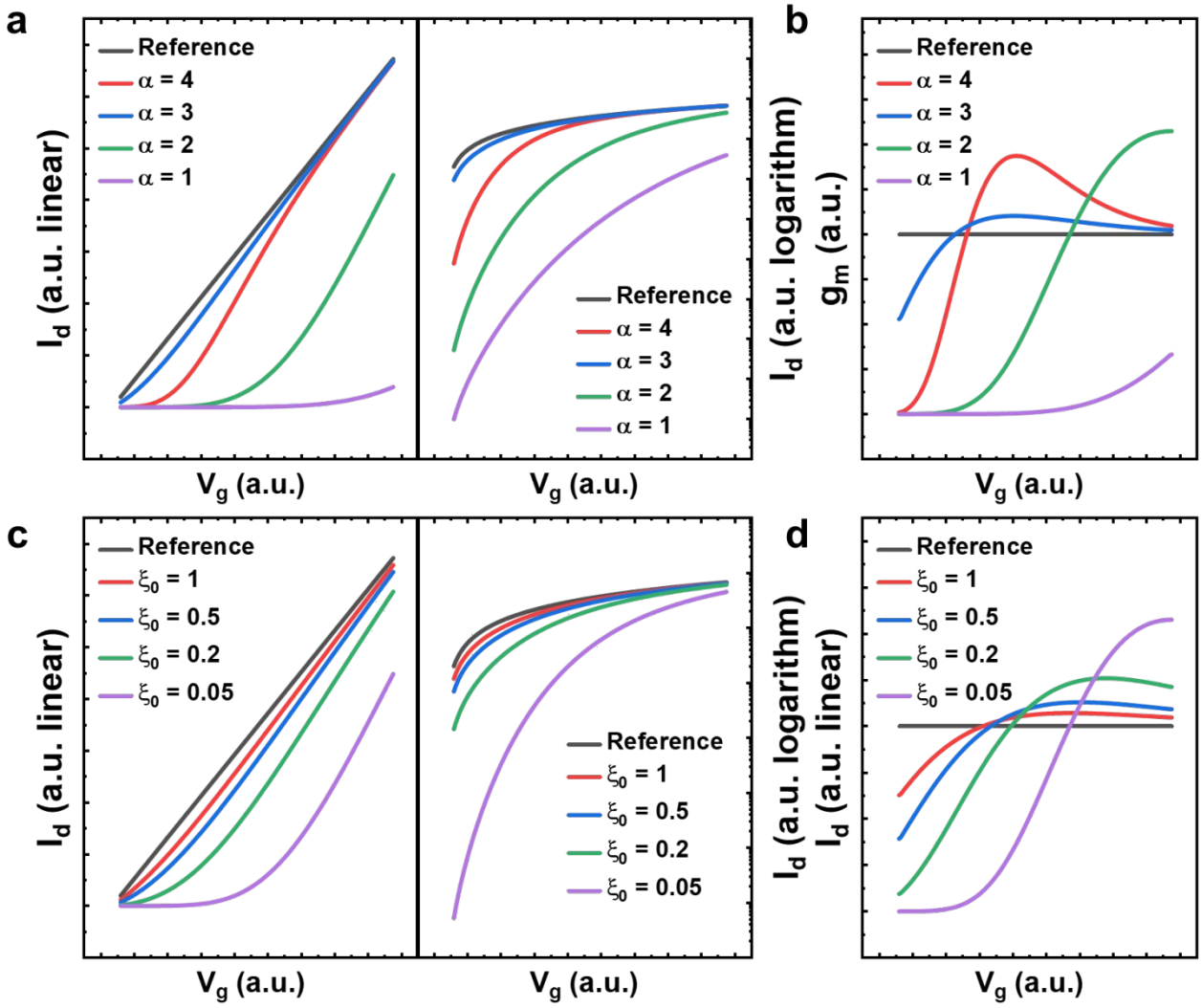

Figure S2. Transfer characteristics and transconductance at different parameters. a, Transfer characteristics plotted on linear and logarithmic scales for different values of α, showing that faster gate modulation of the localization length yields device characteristics approaching ideal performance. **b**, corresponding g_m curves at different α. **c**, Transfer characteristics plotted on linear and logarithmic scales for different initial localization lengths (ξ_0), indicating that larger ξ_0 results in improved device performance closer to the ideal case. **d**, Corresponding g_m plot at different ξ_0.

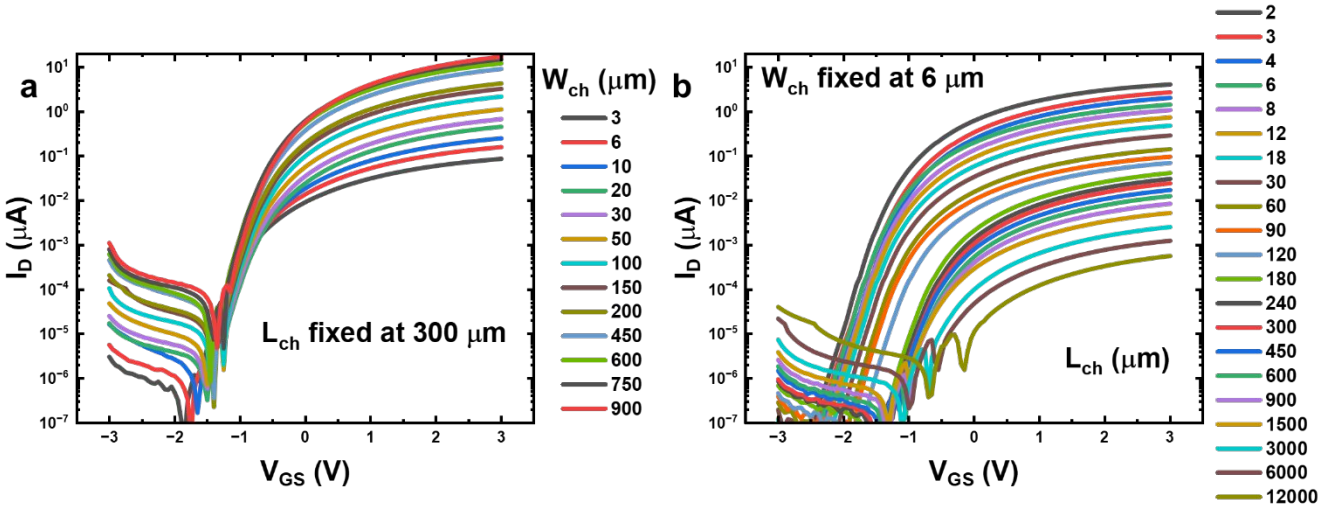

Figure S3. Electron localization in large millimeter-scale devices. a, Channel-width-dependent transfer characteristics with W_{ch} ranging from 3 μm to 900 μm. The small threshold-voltage shift indicates that channel width plays a less significant role than channel length in electron localization. **b**, Channel-length-dependent transfer characteristics with L_{ch} ranging from 2 μm to 12 000 μm. The similar V_{th} shift observed across all lengths, consistent with the main-text discussion, confirms that localization originates from intrinsic channel material properties. The influence of contact resistance is negligible in these long-channel devices.

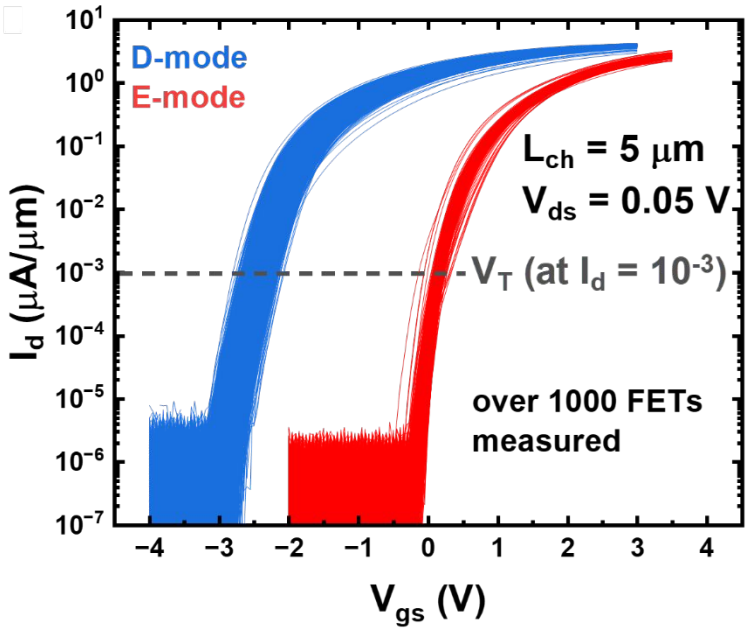

Figure S4. Statistical Transfer Characterizations. Statistical transfer characteristics of over 1000 FETs with a channel length of 5 μm, demonstrating minimal device-to-device variation.

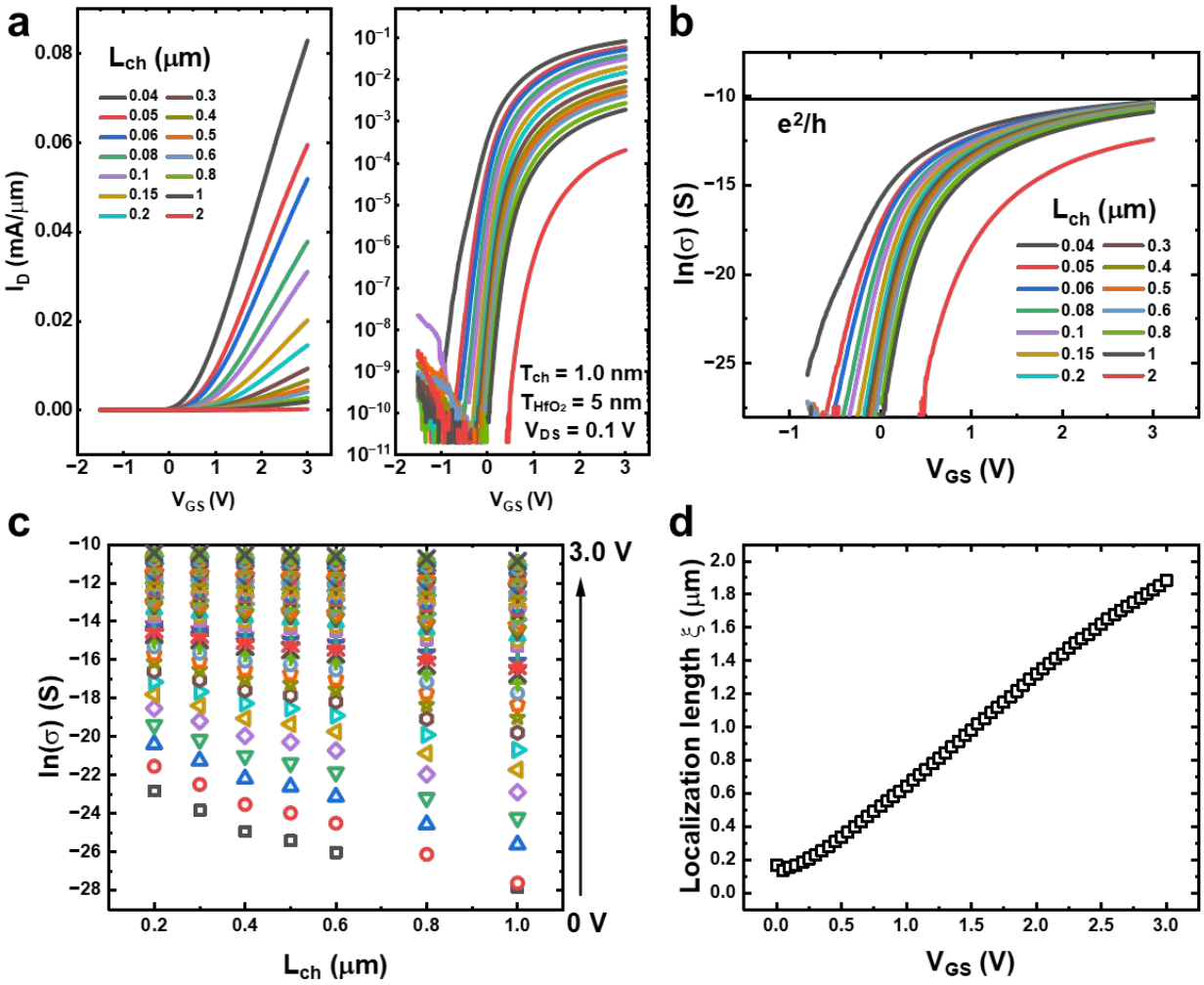

Figure S5. Electron localization in 1.0 nm thick In_2O_3. a, Transfer characteristics of In_2O_3 FETs with a 1.0 nm channel thickness with no post O_2 annealing, shown on both linear and logarithmic scales. **b**, Gate-voltage dependence of the normalized conductivity for different channel lengths. **c**, Channel-length-dependent conductivity scaling exhibiting an exponential decrease. **d**, Gate-voltage-dependent localization length extracted from the data in **c**.

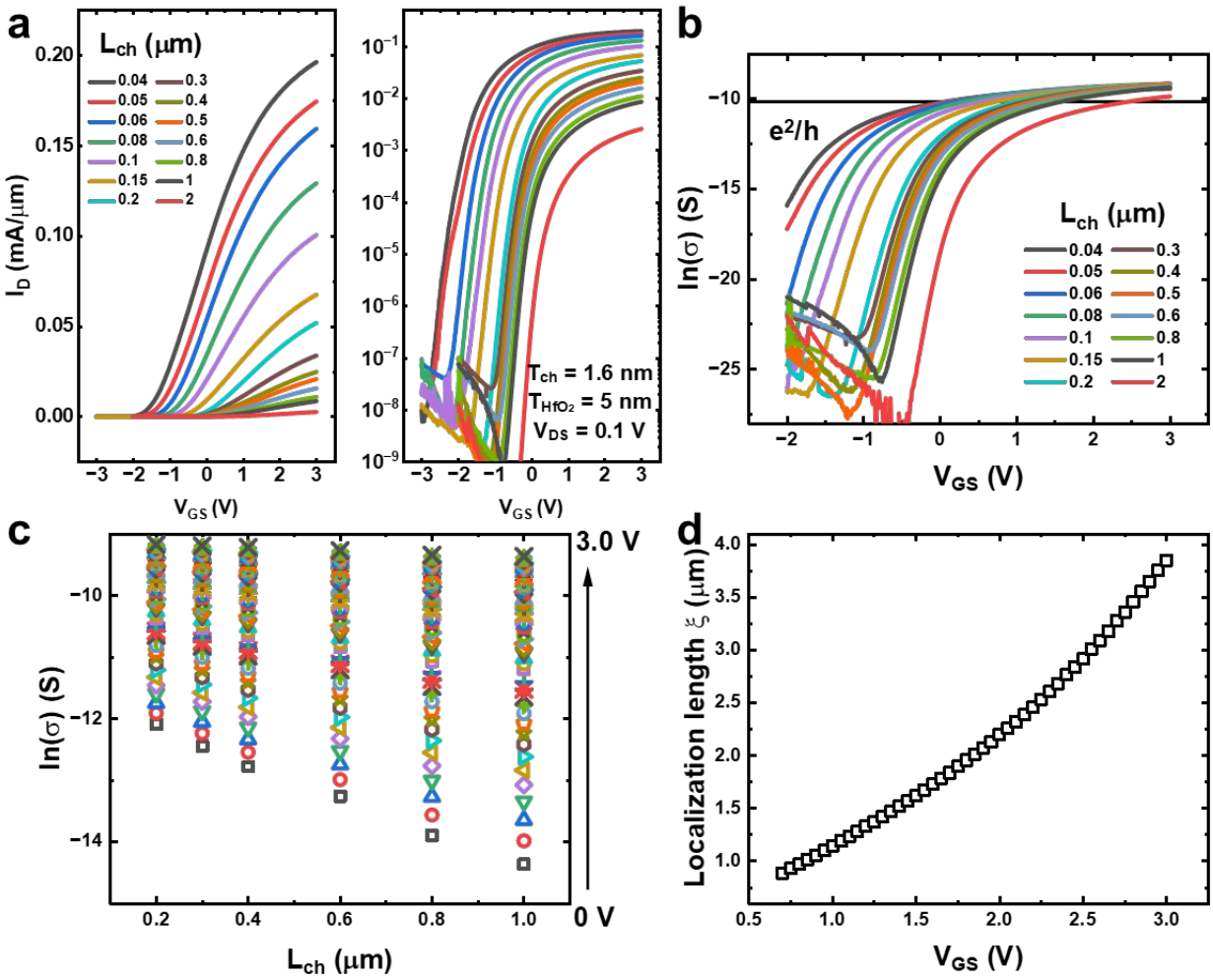

Figure S6. Electron localization in 1.6 nm thick In_2O_3. a, Transfer characteristics of In_2O_3 FETs with a 1.6 nm channel thickness with no post O_2 annealing, shown on both linear and logarithmic scales. **b**, Gate-voltage dependence of the normalized conductivity for different channel lengths. **c**, Channel-length-dependent conductivity scaling exhibiting an exponential decrease. **d**, Gate-voltage-dependent localization length extracted from the data in **c**.

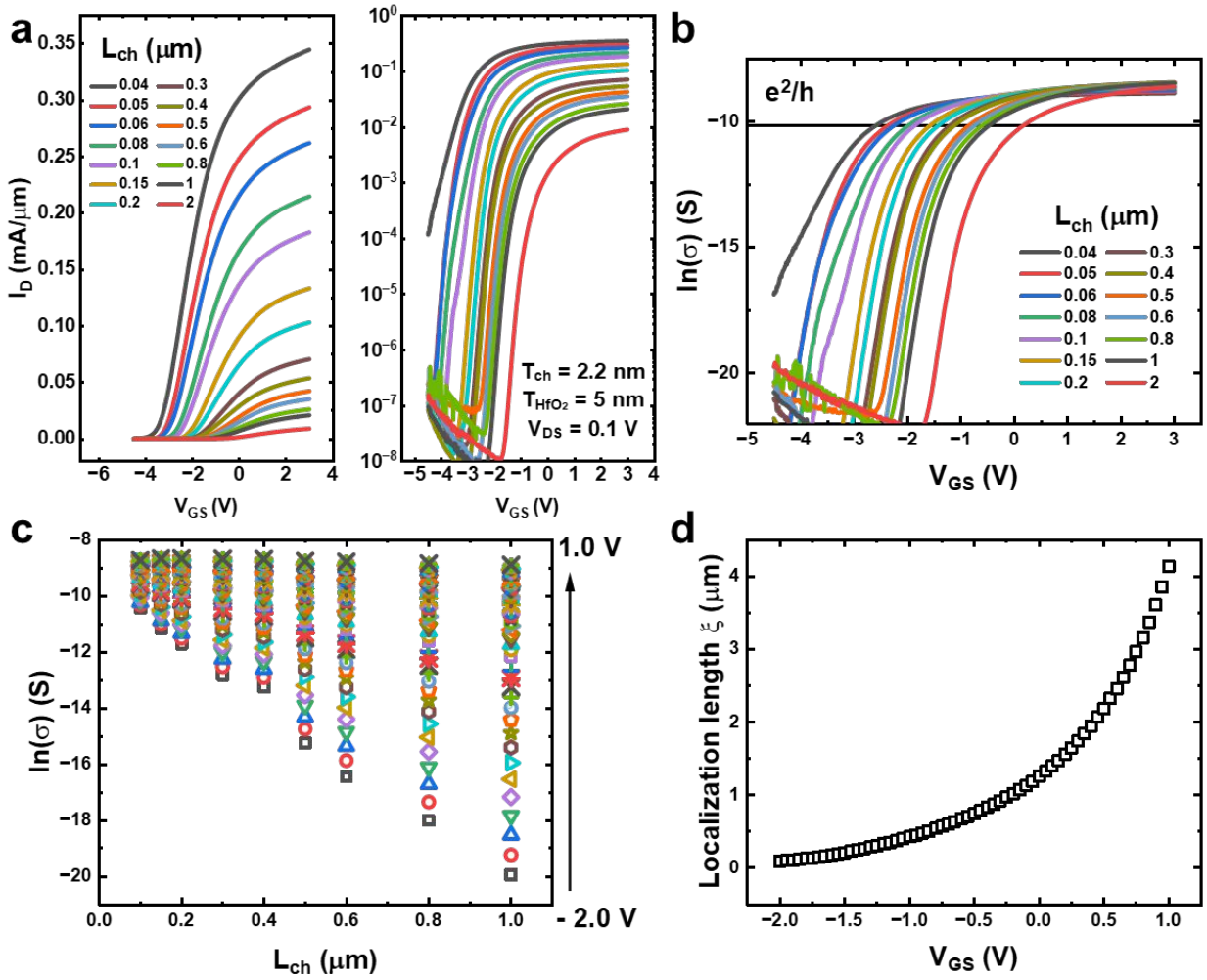

Figure S7. Electron localization in 2.2 nm thick In_2O_3. a, Transfer characteristics of In_2O_3 FETs with a 2.2 nm channel thickness with no post O_2 annealing, shown on both linear and logarithmic scales. **b**, Gate-voltage dependence of the normalized conductivity for different channel lengths. **c**, Channel-length-dependent conductivity scaling exhibiting an exponential decrease. **d**, Gate-voltage-dependent localization length extracted from the data in **c**.

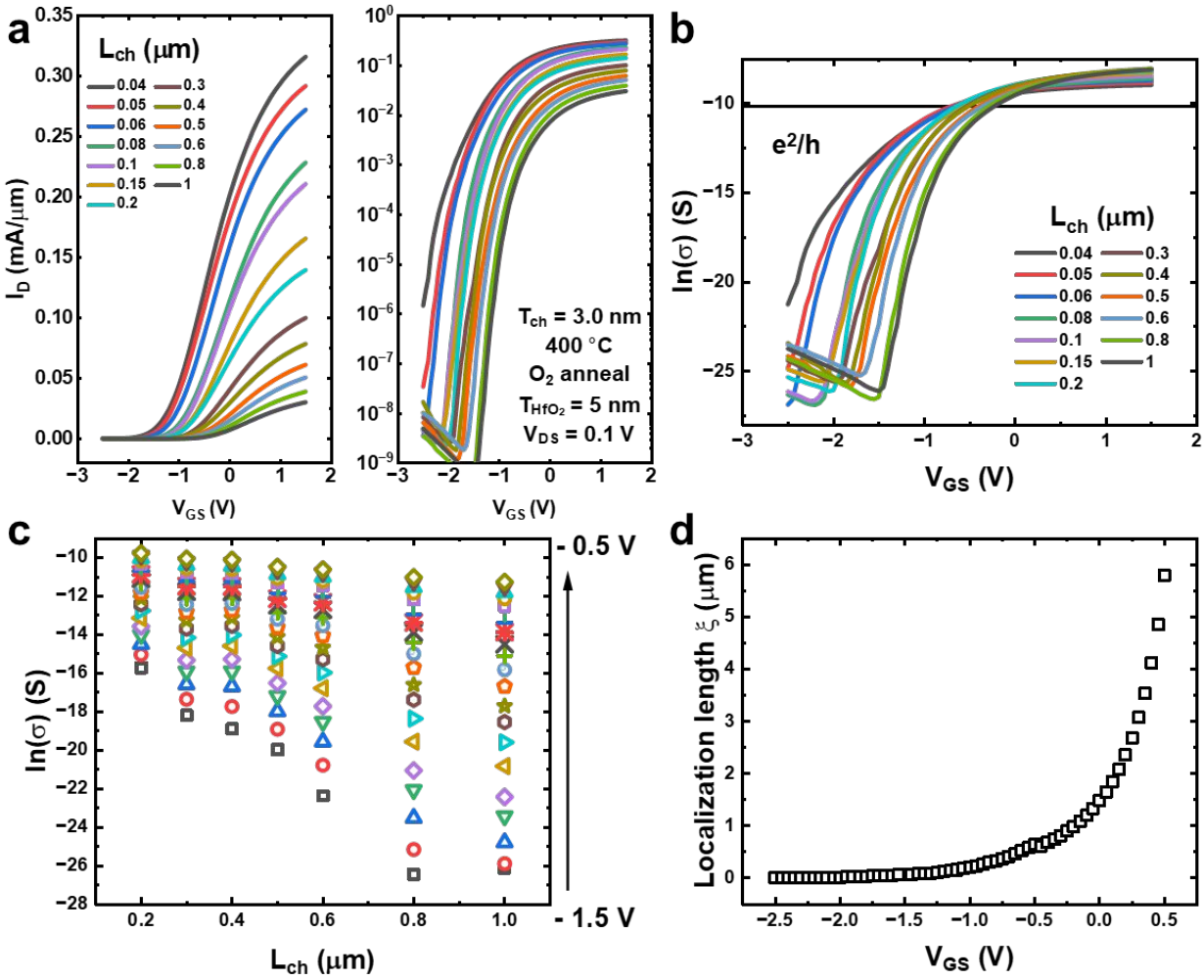

Figure S8. Electron localization in 3.0 nm thick In_2O_3 with 400 °C O_2 annealing. a, Transfer characteristics of In_2O_3 FETs with a 3.0 nm channel thickness with post O_2 annealing at 400 °C, shown on both linear and logarithmic scales. **b**, Gate-voltage dependence of the normalized conductivity for different channel lengths. **c**, Channel-length-dependent conductivity scaling exhibiting an exponential decrease. **d**, Gate-voltage-dependent localization length extracted from the data in **c**.

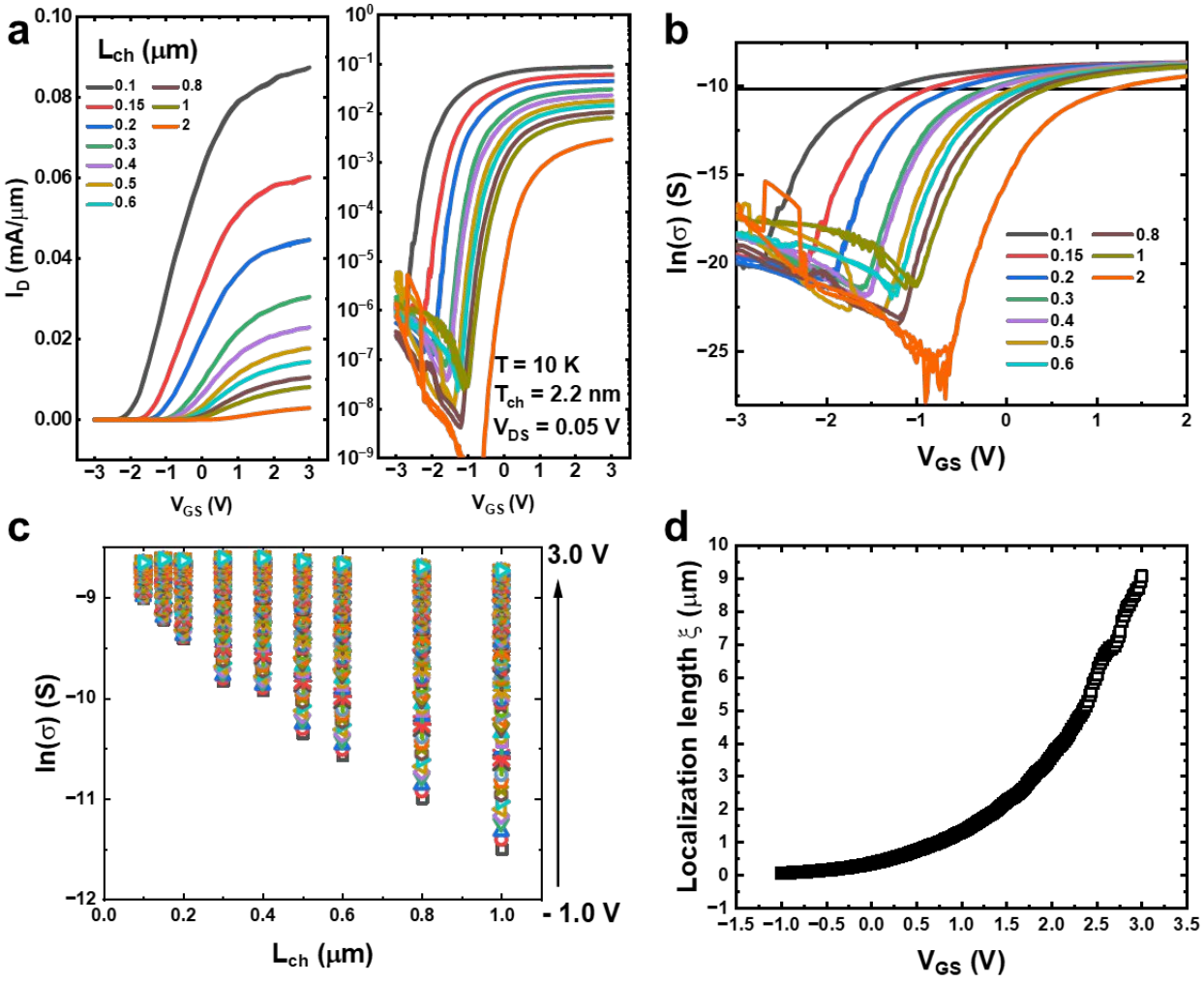

Figure S9. Electron localization in 2.2 nm thick In_2O_3 at 10 K. a, Transfer characteristics of In_2O_3 FETs with a 2.2 nm channel thickness with no post O_2 annealing measured at 10 K, shown on both linear and logarithmic scales. **b**, Gate-voltage dependence of the normalized conductivity for different channel lengths. **c**, Channel-length-dependent conductivity scaling exhibiting an exponential decrease. **d**, Gate-voltage-dependent localization length extracted from the data in **c**.

Supplementary notes:

Note S1: Degree of disorder in different dimensions.

The mean free path is:

$$l = v_F \tau \ (1)$$

where $v_F = \hbar k_F / m^*$ is the Fermi velocity and τ is the relaxation time.

Mobility is:

$$\mu = \frac{e\tau}{m^*} \ (2)$$

Combine them:

$$l = \frac{\hbar k_F \mu}{e} \ (3)$$

Carrier density in different dimensions:

$$n_{1D} = \frac{g_s g_v k_F}{\pi},\ n_{2D} = \frac{g_s g_v {k_F}^2}{4\pi},\ n_{3D} = \frac{g_s g_v {k_F}^3}{6\pi^2} \ (4)$$

Substitute into $k_F l$:

$$k_F l = \frac{\hbar\mu}{e}\left(\frac{\pi n_{1D}}{g_s g_v}\right)^2,\ \frac{\hbar\mu}{e}\left(\frac{4\pi n_{2D}}{g_s g_v}\right) = \frac{4\pi\hbar}{e^2}\sigma_{\square},\ \frac{\hbar\mu}{e}\left(\frac{6\pi^2 n_{3D}}{g_s g_v}\right)^{\frac{2}{3}} \ (5)$$

where $\sigma_{\square} = e n_{2D} \mu$